Journal of Molecular Spectroscopy **202,** 67–82 (2000)
doi:10.1006/jmsp.2000.8113, available online at http://www.idealibrary.com on IDEAL®

High-Temperature Infrared Measurements in the Region of the Bending Fundamental of $H^{12}C^{14}N$, $H^{12}C^{15}N$, and $H^{13}C^{14}N$

A. G. Maki,* G. Ch. Mellau,† S. Klee,† M. Winnewisser,† and W. Quapp‡

**15012 24 Ave. S.E., Mill Creek, Washington 98012; †Physikalisch-Chemisches Institut, Justus-Liebig-Universität Gießen, Heinrich-Buff-Ring 58, D-35392 Gießen, Germany; and ‡Mathematisches Institut, Universität Leipzig, Augustus-Platz 10-11, D-04109 Leipzig, Germany*

Received December 27, 1999; in revised form March 2, 2000

High-resolution measurements have been made on the infrared emission spectrum of $H^{12}C^{14}N$, $H^{12}C^{15}N$, and $H^{13}C^{14}N$ at temperatures on the order of 1370 K. The measurements cover the region 400–850 cm^{-1} with a resolution of 0.006 cm^{-1}. New room-temperature absorption measurements are also reported for $H^{13}C^{14}N$ in the regions, 1200–1500 cm^{-1} and 2500–3700 cm^{-1}. These measurements are combined with earlier measurements to obtain improved values for the rovibrational constants for these three isotopomers. The high temperatures allowed us to measure the bending vibrational levels up to the 0 11^{11} 0 state, at more than 7900 cm^{-1} above the ground vibrational level, for $H^{12}C^{15}N$ and $H^{13}C^{14}N$, and the 0 10^{10} 0 state for $H^{12}C^{14}N$. The Coriolis interaction responsible for the laser transitions of $H^{12}C^{14}N$ and $H^{12}C^{15}N$ has also been observed, for the first time, for $H^{13}C^{14}N$. New r_e values are given using the B_e values found in this paper and in a recent paper on deuterated isotopomers.

Key Words: HCN; bond distances; emission spectra; bending vibrations; isotope shifts; molecular spectra; rovibrational constants; infrared spectra; Coriolis perturbations.

INTRODUCTION

In a recent paper (*1*) we reported the analysis of the high-temperature emission spectrum of $D^{13}C^{15}N$ in which we observed levels up to $v_2 = 12$, $l = 12$, which is nearly 6900 cm^{-1} above the ground state. The present paper is a continuation of that work. We have now measured and analyzed the high-temperature emission spectrum in the ν_2 region for $H^{12}C^{14}N$, $H^{12}C^{15}N$, and $H^{13}C^{14}N$. These new measurements give term values for the bending states up to $v_2 = 10$ and $l = 10$ in all three cases and up to $v_2 = 11$, $l = 11$ for $H^{12}C^{15}N$ and $H^{13}C^{14}N$. The smallest l-values were not observed beyond $v_2 = 9$ because of the less favorable intensity factors and the more crowded spectral region where those transitions occur. In addition to observing high v_2 levels, the present measurements also extend to high rotational levels, thus giving better estimates of the higher order centrifugal distortion constants, H_v. Even though there is a high correlation with other constants, we have observed the l-dependence of the l-type resonance constant, represented by q_l.

In an earlier paper (*2*) we presented an analysis of the vibrational energy levels of $H^{12}C^{14}N$ and $H^{12}C^{15}N$ that included some measurements through $v_2 = 6$. In Tables 1–4 of that paper we presented a number of constants that were not measured, but were based on a modest extrapolation of the vibrational dependence of the rovibrational constants. The present measurements vindicate our optimism for the accuracy of those extrapolations and extend our accurate knowledge of the bending potential for three isotopomers of HCN to levels that are well above the ground state of the HNC isomer.

Supplementary data for this article are available on the journal home page (http://www.academicpress.com/jms) and as part of the Ohio State University Molecular Spectroscopy Archives (http://msa.lib.ohio-state.edu/jmsa_hp.htm).

EXPERIMENTAL DETAILS

Most of the details of the high-temperature measurements were presented in Ref. (*1*). Table 1 lists the conditions used in the recording of the emission spectra used in this work. The emission spectra had a resolution, 0.006 cm^{-1}, that was somewhat larger than the Doppler width of 0.0036 cm^{-1} at 1370 K and 700 cm^{-1}. Most of the absorption measurements were taken from spectra used in our earlier papers (*2, 3*). Tables 2, 3, and 4 give the vibrational transitions that were included in the least-squares fits used for this paper.

The calibration of all the emission measurements made use of the ν_2 transitions for $H^{12}C^{14}N$ that had previously been reported (*2, 3*). For the isotopically enriched samples there was sufficient residual $H^{12}C^{14}N$ in the sample to allow such calibration. The accuracy of the calibration was checked by comparing the present values for the vibrational levels with those values given from absorption measurements in our earlier paper (*2*). Especially useful is the comparison of the present value for the 03^10 level with that reported earlier from absorption measurements that were calibrated with the very precisely known CO absorption lines (*4*). A similar comparison was made for the present emission and absorption measurements for $H^{13}C^{14}N$. We believe that the accuracy of the energy levels measured in the emission spectra is well represented by the uncertainties given in the present tables. Energy levels above 3500 cm^{-1} and measured only in absorption spectra were not so thoroughly checked and may have additional calibration errors which lead to uncertainties on the order of ± 0.0008 cm^{-1} at 5000 cm^{-1} and rising to twice that value at 10 000 cm^{-1}.

0022-2852/00 $35.00

TABLE 1
Parameters of the FTS Spectral Emission Measurements

Filename	ZHCNEWS	ZHCNEVS	ZHCNEUS
Species	$H^{12}C^{14}N$	$H^{13}C^{14}N$	$H^{12}C^{15}N$
Region (cm^{-1})	400-855	420-860	400-860
Date (D/M/Y)	2/2/97	1/2/97	31/1/97
Pressure (mbar)	2.9	3.0	3.38
Temperature (K)	1370	1370	1370
Pathlength (cm) of heated region	60	60	60
Aperture diameter (mm)	3.15	3.15	3.15
Resolution (1/MOPD) (cm^{-1})	0.0061	0.0061	0.0061
Bandpass opt. filter (cm^{-1})	400-900(4K)	400-900(4K)	400-900(4K)
High pass el. filter (cm^{-1})	197	197	197
Low pass el. filter (cm^{-1})	1027	1027	1027
Scans coadded	992	1200	850
Highest S/N (rms)	~400	~400	~400
Detector	Ge:Cu (4K)	Ge:Cu (4K)	Ge:Cu (4K)
Windows	KBr	KBr	KBr
Beamsplitter	KBr	KBr	KBr
Focal length of collimator (mm)	418	418	418
Scanner velocity (cm/s)	1.266	1.266	1.266

ANALYSIS OF THE SPECTRA

Based on earlier measurements of the bending manifolds for $H^{12}C^{14}N$ and $H^{12}C^{15}N$ that extended to $v_2 = 6$, it was quite easy to assign the strongest transitions to levels that had already been observed. From the constants given in Tables 7–10 in Ref. (*2*) it was then possible to calculate the transitions for the next higher bending level. After the discovery and analysis of the transitions for each new vibrational level was completed, a new set of constants was determined and used to predict the location of the next higher level. As long as the extrapolation was not more than one unit in the bending quantum number, v_2, the calculated transition wavenumbers were always within 0.04 cm^{-1} of the observed transitions and usually within 0.02 cm^{-1}.

A similar procedure was followed for $H^{13}C^{14}N$ except that we began with much less information about the lower bending vibrations. Before analyzing the emission spectrum of $H^{13}C^{14}N$, we measured and analyzed the absorption spectrum in the region of the $2\nu_2$ band. Those measurements provided information on bending levels through $v_2 = 5$. Absorption spectra also were measured for the $3\nu_2$ and $\nu_2 + \nu_3$ regions, which gave more data for the bending manifold as well as for the transitions involving ν_3 through the $03^{1,3}1$ levels. In the emission spectra we could identify transitions for all those levels and then could extend the assignments to higher levels using the "boot-strap" iterative technique just described for extending the transitions for $H^{12}C^{14}N$.

As can be seen in Fig. 1 the emission spectrum was quite crowded, especially in the region 700–725 cm^{-1} where there were many *Q*-branch transitions. Also visible in Fig. 1 are the *Q*-branch absorption lines of the $01^{1f}0$–$00^{0}0$ transitions that come from the cool portion of the absorption cell near the windows. In fact, most of the emission lines in the region from 712 to 715 cm^{-1} are obscured by the strong self-absorption of the transitions from the ground state. Figure 2 shows the emission spectrum in the *R*-branch region where the density of lines is not nearly so great. Even in such a region of comparatively low line density, there are several lines that are not well resolved from other lines.

To some extent the success of finding transitions was dependent on accidents of fate. If a long stretch of transitions should fall under some stronger transitions, then it was not possible to be certain of the assignment of the few transitions that could be resolved and we chose to ignore those assignments. That is the primary reason that the same levels were not observed for all isotopic species, even though the emission spectra were measured under comparable conditions of temperature, path length, and pressure.

In our earlier measurements on $D^{13}C^{15}N$ (*1*) we showed that the strongest transitions were of the type $v_2 + 1$, $l + 1$, $J + 1 \rightarrow v_2$, $l = v_2$, J. Fortunately for this study, those transitions were mostly in a region of the spectrum where the density of lines was comparatively low. Those were the main factors that allowed us to observe such high vibrational levels with $v_2 = l$. Figure 3 shows an overview of a region of the spectrum of $H^{12}C^{15}N$ that contains three series of *Q*-branch transitions of the type $v_2 + 1$, $l + 1 \rightarrow v_2$, $l = v_2$. The figure shows the rapid decline in intensity with increasing values of v_2. It also illustrates the change in ΔB for the *Q* branches as v_2 increases.

The present measurements were analyzed in the same way as our earlier measurements (*1, 2*). For each isotopomer, all the present measurements were combined with previous measurements in a single least-squares fit that gave the values and uncertainties for the rovibrational constants for each vibrational state as corrected for the effects of *l*-type resonance and for any Coriolis resonances that produce directly observed displacements of some lines.

The least-squares fit used an energy matrix with the diagonal matrix elements

$$\langle v_1, v_2, v_3, l, J|\mathbf{H}/hc|v_1, v_2, v_3, l, J\rangle = T(v, l, J) = G_0(v, l) + F(v, l, J), \quad [1]$$

where the unperturbed rotational term value is given by

$$F(v, l, J) = B_v[J(J+1) - l^2] - D_v[J(J+1) - l^2]^2 + H_v[J(J+1) - l^2]^3, \quad [2]$$

and the unperturbed vibrational term value is given by $G_0(v, l)$. The effects of *l*-type resonance were taken into account by using off-diagonal matrix elements of the form

$$\begin{aligned}\langle v_1, v_2, v_3, l, J|\mathbf{H}/hc|v_1, v_2, v_3, l \pm 2, J\rangle &= \tfrac{1}{4}[q_v - q_{vJ}J(J+1) + q_{vJJ}J^2(J+1)^2 + q_l(l \pm 1)^2] \\ &\times \{(v_2 \mp l)(v_2 \pm l + 2)[J(J+1) - l(l \pm 1)] \\ &\times [J(J+1) - (l \pm 1)(l \pm 2)]\}^{1/2}\end{aligned} \quad [3]$$

TABLE 2
Wavenumbers of Band Centers in cm^{-1} for the Infrared Bands of $H^{12}C^{14}N$ Used in the Present Analysis

transition	ν_c	transition	ν_c	transition	ν_c
01^10-00^00	711.979 569(18)†*[a]	07^30-06^40	651.568 31(43)*	01^12-01^10	4166.315 480(65)†
02^00-00^00	1411.413 375(26)†	07^50-06^40	713.288 28(30)*	02^02-00^00	5571.733 697(123)†
02^20-00^00	1426.529 865(23)†	07^70-06^60	729.035 46(47)*	02^02-01^10	4859.754 129(113)†
02^00-01^10	699.433 806(23)†*	08^00-07^10	669.125 58(47)*	02^22-01^10	4874.085 599(127)†
02^20-01^10	714.550 296(18)†*	08^20-07^10	684.691 31(101)*	00^03-00^00	6228.598 297(116)†
03^10-00^00	2113.450 489(23)†	08^40-07^30	700.435 16(72)*	01^13-01^10	6218.058 07(55)†
03^30-00^00	2144.760 711(54)†	08^60-07^50	716.316 36(122)*	10^00-00^00	3311.476 829(49)†
03^10-01^10	1401.470 920(25)†	08^80-07^70	732.251 73(45)*	10^00-01^10	2599.497 261(48)†
03^30-01^10	1431.781 142(54)†	09^10-08^00	671.532 85(64)*	10^00-02^00	1900.063 455(52)†
03^10-02^00	702.037 115(30)†*	09^50-08^40	703.302 21(103)*	11^10-00^00	4004.162 281(36)†
03^10-02^20	686.920 624(28)†*	09^70-08^60	719.396 05(134)*	11^10-01^10	3292.182 712(33)†
03^30-02^20	717.230 846(52)†*	09^90-08^80	735.572 55(48)*	11^10-02^00	2592.748 906(34)†
04^00-00^00	2802.958 821(38)†	$010^{10}0-09^90$	738.997 16(269)*	11^10-02^20	2577.632 416(32)†
04^00-01^10	2090.979 252(37)†	00^01-00^00	2096.845 558(27)†	12^00-00^00	4684.310 004(60)†
04^20-01^10	2106.195 973(33)†	00^01-01^10	1384.865 990(30)†	12^20-00^00	4699.208 984(89)†
04^00-02^00	1391.545 446(41)†	01^11-00^00	2805.581 932(47)†	12^00-02^00	3272.896 630(61)†
04^20-02^20	1391.645 677(33)†	01^11-02^00	1394.168 557(51)†	12^20-02^20	3272.679 119(87)†
04^00-03^10	689.508 331(41)†*	01^11-03^10	692.131 442(51)*	12^00-03^10	2570.859 515(61)†
04^20-03^10	704.725 052(39)†*	01^11-00^01	708.736 373(53)*	12^20-03^10	2585.758 495(89)†
04^20-03^30	674.414 831(60)*	02^01-00^00	3502.119 692(61)†	12^20-03^30	2555.448 273(93)†
04^40-03^30	720.020 804(109)†*	02^21-00^00	3516.871 529(60)†	20^00-00^00	6519.610 318(60)†
05^10-00^00	3495.113 952(73)†	02^01-01^10	2790.140 123(61)†	20^00-01^10	5807.630 749(59)†
05^10-01^10	2783.134 383(72)†	02^21-01^10	2804.891 960(58)†	21^10-00^00	7192.763 680(62)†
05^10-02^20	2068.584 087(72)†	02^01-01^11	696.537 760(75)*	21^10-01^10	6480.784 111(59)†
05^30-02^20	2099.142 607(87)†	02^21-01^11	711.289 597(74)*	22^00-01^10	7141.531 402(118)†
05^10-03^10	1381.663 463(74)†	03^11-00^00	4201.205 507(49)†	22^20-01^10	7156.085 601(95)†
05^30-03^30	1381.911 761(98)†	03^11-01^10	3489.225 939(48)†	22^00-02^00	6442.097 596(116)†
05^10-04^00	692.155 132(78)*	03^11-02^00	2789.792 133(51)†	22^20-02^20	6441.535 306(93)†
05^10-04^20	676.938 411(76)*	03^11-02^20	2774.675 642(49)†	23^10-00^00	8516.469 15(22)†
05^30-04^20	707.496 930(91)*	03^31-02^20	2804.307 166(163)†	23^10-03^10	6403.018 66(22)†
05^50-04^40	722.918 549(262)*	03^11-02^01	699.085 816(75)*	23^30-03^30	6401.819 82(36)†
06^00-03^10	2061.158 212(219)†	03^11-02^21	684.333 978(75)*	30^00-00^00	9627.086 85(22)†
06^20-03^10	2076.522 892(174)†	03^31-02^21	713.965 502(167)*	31^10-01^10	9568.383 98(21)†
06^40-03^30	2092.263 340(297)†	04^01-03^11	686.833 54(30)*	20^01-00^00	8585.581 07(12)†
06^00-05^10	679.494 75(21)*	04^21-03^11	701.732 46(43)*	20^01-00^01	6488.735 51(12)†
06^20-05^10	694.859 429(174)*	04^41-03^31	716.763 26(43)*	21^11-00^00	9256.087 09(35)†
06^20-05^30	664.300 909(176)*	05^11-01^10	4865.464 88(36)†	21^11-01^10	8544.107 52(35)†
06^40-05^30	710.351 58(29)*	05^11-04^01	689.405 40(40)*		
06^40-05^50	649.323 99(37)*	05^31-04^21	704.475 21(172)*		
06^60-05^50	725.923 98(37)*	05^51-04^41	719.672 38(99)*		
07^10-06^00	682.079 44(26)*	06^61-05^51	722.720 91(124)*		
07^10-06^20	666.714 76(30)*	00^02-00^00	4173.070 839(77)†		
07^30-06^20	697.618 98(39)*	01^12-00^00	4878.295 049(63)†		

[a] The uncertainty in the last digits (twice the standard deviation) is given in parentheses. An asterisk, *, indicates the band was measured in emission and a dagger, †, indicates the band was measured in absorption.

and

$$\begin{aligned}\langle v_1, v_2, v_3, l, J|\mathbf{H}/hc|v_1, v_2, v_3, l \pm 4, J\rangle \\ = (\rho_v/16)\{(v_2 \mp l)(v_2 \pm l + 2)(v_2 \mp l - 2) \\ \times (v_2 \pm l + 4)[J(J+1) - l(l \pm 1)][J(J+1) \\ - (l \pm 1)(l \pm 2)][J(J+1) - (l \pm 2)(l \pm 3)] \\ \times [J(J+1) - (l \pm 3)(l \pm 4)]\}^{1/2}.\end{aligned} \quad [4]$$

In Eq. [3] we give the q_l term which is equivalent to the q_t^k term described by Watson (5). For HCN the k and l quantum numbers are the same. Although defined somewhat differently, the q_l term is equivalent to the π_{ll} given in Ref. (2). In that earlier work we tried to determine the π_{ll} term from fits of the q_v terms for Σ and Π states. In the present case the l-dependence is built into the energy matrix which is where it really belongs. The value of q_l seems to be fairly well determined although it is highly correlated with ρ_v and both are small off-diagonal constants coupling levels whose separation is many orders of magnitude larger than the coupling constants. For Π vibrational states the coefficient of q_l is zero and so it does not affect the value of q_v for Π states. For $v_2 = 2$ states the q_l term cannot be distinguished from the q_v term. Only for the $v_2 > 2$ states can we hope to determine a value for q_l. In our fits we have used the same value of q_l for all values of v_2.

TABLE 3
Wavenumbers of Band Centers in cm^{-1} for the Infrared Bands of $H^{13}C^{14}N$ Used in the Present Analysis

transition	ν_c	transition	ν_c	transition	ν_c
01^10-00^00	705.965 734(21)†*[a]	07^10-06^00	677.389 49(56)*	03^31-02^20	2763.455 35(32)†
02^00-00^00	1399.760 658(34)†	07^30-06^20	692.754 64(40)*	03^31-05^10	710.441 38(33)*
02^20-00^00	1414.634 469(31)†	07^50-06^40	708.264 99(45)*	03^11-02^01	693.169 534(168)*
02^00-01^10	693.794 924(33)†*	07^70-06^60	723.873 18(31)*	03^31-02^21	707.812 53(31)*
02^20-01^10	708.668 735(27)†*	08^00-07^10	664.721 19(50)*	04^01-02^00	3430.493 92(51)†
03^10-00^00	2096.269 753(27)†	08^40-07^30	695.694 95(86)*	04^21-02^20	3430.282 29(55)†
03^30-00^00	2126.119 952(84)†	08^60-07^50	711.424 25(57)*	04^01-03^11	681.294 38(51)*
03^10-01^10	1390.304 019(27)†	08^80-07^70	727.244 78(43)*	04^21-03^11	695.956 57(55)*
03^10-02^00	696.509 095(37)*	09^70-08^60	714.668 13(129)*	04^41-03^31	710.776 38(47)*
03^30-02^20	711.485 483(80)*	09^90-08^80	730.723 88(69)*	05^31-04^21	3271.505 828(104)†
04^00-00^00	2780.585 370(52)†	010^80-09^70	717.997 20(101)*	05^51-04^41	3271.336 366(128)†
04^00-01^10	2074.619 636(51)†	$010^{10}0-09^90$	734.308 64(86)*	10^00-00^00	3293.513 232(117)†
04^20-01^10	2089.618 040(49)†	$011^{11}0-010^{10}0$	737.996 80(159)*	11^10-01^10	3274.806 456(63)†
04^00-02^00	1380.824 711(51)†	00^01-00^00	2063.047 099(46)†	11^10-02^00	2581.011 532(71)†
04^20-02^20	1380.949 304(49)†	00^01-01^10	1357.081 366(43)†	11^10-02^20	2566.137 721(68)†
04^00-03^10	684.315 617(53)*	01^11-00^00	2765.304 460(75)†	12^00-02^00	3256.079 946(165)†
04^20-03^10	699.314 021(53)*	01^11-01^10	2059.338 727(75)†	12^20-02^20	3255.874 415(165)†
04^40-03^30	714.415 459(131)*	01^11-02^00	1365.543 802(80)†	13^10-03^10	3237.154 33(32)†
05^10-00^00	3467.648 439(110)†	01^11-02^20	1350.669 991(79)†	13^30-03^30	3236.695 40(57)†
05^10-01^10	2761.682 705(109)†	01^11-00^01	702.257 361(82)*	00^02-00^00	4105.875 00(63)†
05^10-02^00	2067.887 781(109)†	02^01-00^00	3455.790 658(78)†	01^12-00^00	4804.177 75(28)†
05^30-02^20	2083.158 357(132)†	02^21-00^00	3470.277 294(95)†	20^00-00^00	6483.281 24(21)†
05^10-03^10	1371.378 686(109)†	02^01-01^10	2749.824 924(79)†	21^10-01^10	6445.692 88(22)†
05^30-03^30	1371.672 874(141)†	02^21-01^10	2764.311 560(93)†	22^00-02^00	6408.201 54(89)†
05^10-04^00	687.063 069(108)*	02^21-03^10	1374.007 541(97)†	22^20-02^20	6407.642 25(126)†
05^30-04^20	702.209 053(134)*	02^21-04^00	689.691 924(106)*	10^01-00^00	5343.658 669(156)†
05^50-04^40	717.457 500(151)*	02^01-00^01	1392.743 558(88)†	11^11-00^00	6027.345 82(21)†
06^00-05^10	674.707 87(21)*	02^01-01^11	690.486 197(105)*	11^11-01^10	5321.380 09(21)†
06^20-05^10	689.876 43(25)*	02^21-01^11	704.972 833(113)*	12^01-00^00	6699.101 06(42)†
06^40-05^30	705.193 10(24)*	03^11-01^10	3442.994 457(154)†	20^01-00^00	8519.244 37(100)†
06^60-05^50	720.610 309(196)*	03^11-02^00	2749.199 533(157)†	30^00-00^00	9571.696 40(57)†

[a] The uncertainty in the last digits (twice the standard deviation) is given in parentheses. An asterisk, *, indicates the band was measured in emission and a dagger, †, indicates the band was measured in absorption.

The value of ρ_v was even better determined than q_l and so it was possible to obtain a rough estimate of the vibrational dependence of ρ_v.

In keeping with the notation used in our most recent paper (*1*), we report the energy levels in terms of $G_0(v, l)$, where $G_0(0, 0) = 0$, but the observed band centers are given by

$$\nu_c = G_c(v, l)' - G_c(v, l)'', \qquad [5]$$

where

$$G_c(v, l) = G_0(v, l) - B_v l^2 - D_v l^4 - H_v l^6. \qquad [6]$$

Note that this definition of $G_c(v, l)$ is nearly the same as the G_v given in Ref. (*2*).

In this analysis no vibrational resonances have been analyzed and so such matrix elements have not been used in the energy matrix. A single type of Coriolis interaction has been found for these three isotopomers and was represented by the off-diagonal matrix element

$$\langle v_1, v_2, v_3, l, J|\mathbf{H}/hc|v_1, v_2 + 3, v_3 - 1, l \pm 1, J\rangle = [W_v + W_{vJ}J(J + 1)][J(J + 1) - l(l \pm 1)]^{1/2}. \qquad [7]$$

In our least-squares fit of the data for $H^{13}C^{14}N$ we have combined all the data available to us in a single fit that had over 8200 measurements. Included in the fit were the rotational transitions measured earlier (*6–8*). Each set of measurements, or in some cases each measurement, was weighted by the inverse square of the measurement uncertainty. Many of the transitions were unresolved doublets and in those cases our program fits the unresolved doublets to the average position of the two transitions.

For the fits of the $H^{12}C^{14}N$ and $H^{12}C^{15}N$ data we included most of our earlier infrared measurements (*2, 3*), but some vibrational levels that were not involved in the high-temperature measurements were left out of the fit. A total of 12 200 measurements were included in the $H^{12}C^{14}N$ least-squares fit and 7800 measurements in the $H^{12}C^{15}N$ fit.

The rovibrational constants that resulted from the fits are given in Tables 5–8. In certain cases the data were not extensive enough to determine the values for some higher order

TABLE 4
Wavenumbers of Band Centers in cm^{-1} for the Infrared Bands of $H^{12}C^{15}N$ Used in the Present Analysis

transition	ν_c	transition	ν_c	transition	ν_c
01^10-00^00	711.026 554(22)†*[a]	07^10-02^00	3439.672 19(26)†	03^31-06^20	12.524 49(27)[b]
02^00-00^00	1409.306 512(37)†	07^10-06^00	680.991 569(191)*	04^01-02^00	3442.528 195(161)†
02^20-00^00	1424.759 050(35)†	07^10-06^20	665.296 64(28)*	04^21-02^20	3442.258 870(167)†
02^00-01^10	698.279 958(35)†*	07^30-06^20	696.859 47(36)*	04^01-03^11	685.820 104(183)*
02^20-01^10	713.732 496(31)†*	07^50-06^40	712.846 00(21)*	04^21-03^11	701.003 317(185)*
03^10-00^00	2110.330 492(35)†	07^70-06^60	728.902 68(21)*	04^41-03^31	716.325 21(46)*
03^30-00^00	2141.308 510(61)†	08^00-07^10	667.863 47(84)*	10^00-00^00	3310.089 147(86)†
03^10-01^10	1399.303 938(34)†	08^40-07^30	699.823 32(51)*	10^00-01^10	2599.062 593(86)†
03^30-01^10	1430.281 956(58)†	08^60-07^50	716.006 64(36)*	11^10-01^10	3290.813 166(65)†
03^10-02^00	701.023 980(43)*	08^80-07^70	732.255 38(24)*	11^10-02^00	2592.533 208(72)†
03^10-02^20	685.571 442(39)*	09^50-08^40	702.840 98(73)*	11^10-02^20	2577.080 670(70)†
03^30-02^20	716.549 460(57)*	09^70-08^60	719.247 75(46)*	12^00-02^00	3271.505 828(104)†
04^00-00^00	2798.635 100(66)†	09^90-08^80	735.710 98(44)*	12^20-02^20	3271.336 366(128)†
04^00-01^10	2087.608 546(65)†	010^80-09^70	722.566 67(106)*	13^10-03^10	3252.029 959(154)†
04^20-01^10	2103.157 600(59)†	$010^{10}0-09^90$	739.267 86(96)*	13^30-03^30	3251.633 29(22)†
04^00-02^00	1389.328 588(66)†	$011^{11}0-010^{10}0$	742.923 88(167)*	00^02-00^00	4108.640 17(112)†
04^20-02^20	1389.425 104(58)†	00^01-00^00	2064.316 173(47)†	01^12-00^00	4813.162 01(91)†
04^00-03^10	688.304 608(67)*	00^01-01^10	1353.289 619(46)†	20^00-00^00	6725.247 18(91)†
04^20-03^10	703.853 662(60)*	01^11-00^00	2772.221 969(48)†	21^10-01^10	6477.771 658(164)†
04^20-03^30	672.875 644(71)*	01^11-01^10	2061.195 415(45)†	22^00-02^00	6439.125 3(31)†
04^40-03^30	719.476 219(126)*	01^11-00^01	707.905 797(64)*	22^20-02^20	6438.619 9(27)†
05^10-01^10	2778.706 252(87)†	02^01-00^00	3467.783 161(79)†	10^01-00^00	5360.254 347(166)†
05^30-02^20	2096.193 130(124)†	02^01-01^10	2756.756 607(80)†	11^11-00^00	6049.010 01(52)†
05^30-03^30	1379.643 669(125)†	02^21-01^10	2771.784 170(96)†	11^11-01^10	5337.983 46(52)†
05^10-04^00	691.097 707(93)*	02^01-01^11	695.561 191(89)*	12^01-00^00	6725.247 18(91)†
05^10-04^20	675.548 653(91)*	02^21-01^11	710.588 755(101)*	20^01-00^00	8551.184 27(68)†
05^30-04^20	706.768 026(116)*	03^11-01^10	3454.988 049(95)†	30^00-00^00	9621.739 54(112)†
05^30-04^40	660.167 450(138)*	03^11-02^00	2756.708 091(99)†		
05^50-04^40	722.511 469(161)*	03^11-02^20	2741.255 553(99)†		
06^00-05^10	678.254 33(21)*	03^31-02^20	2771.447 509(196)†		
06^20-05^10	693.949 262(169)*	03^11-02^01	698.231 442(121)*		
06^40-05^30	709.765 897(191)*	03^11-02^21	683.203 879(133)*		
06^60-05^50	725.654 213(131)*	03^31-02^21	713.395 835(199)*		

[a] The uncertainty in the last digits (twice the standard deviation) is given in parentheses. An asterisk, *, indicates the band was measured in emission and a dagger, †, indicates the band was measured in absorption.
[b] laser transitions

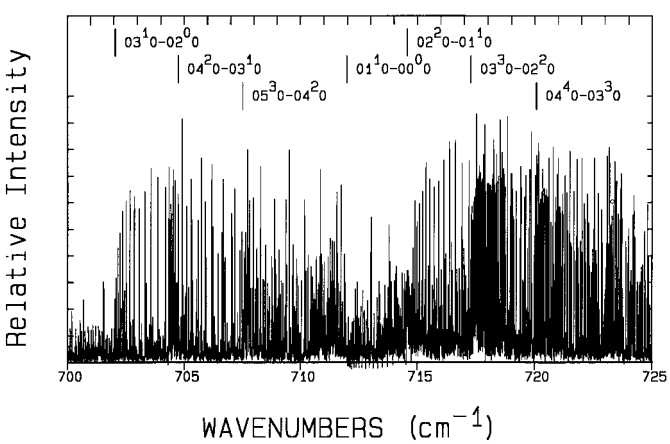

FIG. 1. The emission spectrum near the center of the band for $H^{12}C^{14}N$. Note the weak self-absorption lines directed downward between 712 and 714 cm^{-1}. The first lines of several *Q* branches are indicated at the top of the figure.

constants. Those constants that are given in square brackets were fixed at values extrapolated from the rovibrational dependence of other vibrational states. We believe that such extrapolated values are better than fixing the constants at some arbitrary value such as zero.

NEW RESONANCES THAT HAVE BEEN FOUND

Coriolis Resonances

For $H^{12}C^{14}N$ and $H^{12}C^{15}N$ it has previously been shown that there is a Coriolis interaction that couples levels such as 01^11 and 04^00, or 02^01 and $05^{1e}0$. That interaction is represented by the matrix element given above in Eq. [7]. Tables 5 and 6 of Ref. (*2*) give a good description of the Coriolis perturbations found for $H^{12}C^{14}N$ and $H^{12}C^{15}N$. The present measurements give constants that are only slightly different, always within the uncertainty of the constants. A few new level crossings have been identified and those are given in Table 9. As was done in

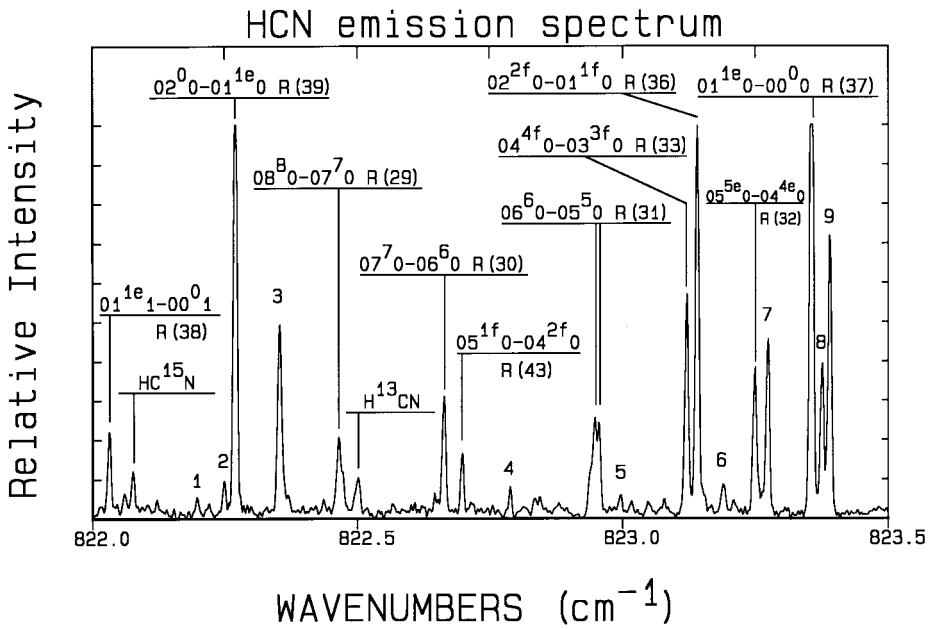

FIG. 2. The emission spectrum of the *R*-branch region for $H^{12}C^{14}N$. The numbered lines have been identified as follows: 1, $05^{5e}1$–$04^{4e}1$ $R(33)$; 2, $03^{1e}1$–$02^{0}1$–$02^{0}1$ $R(42)$; 3, $010^{10}0$–$09^{9}0$ $R(27)$ and $09^{9}0$–$08^{8}0$ $R(28)$; 4, $07^{5e}0$–$06^{4e}0$ $R(35)$; 5, $02^{2e}1$–$01^{1e}1$ $R(33)$; 6, $03^{3e}1$–$02^{2e}1$ $R(36)$; 7, $02^{2e}0$–$01^{1e}0$ $R(32)$; 8, $05^{5f}0$–$04^{4f}0$ $R(32)$; and 9, $03^{1e}0$–$02^{0}0$ $R(41)$.

Table 5 of Ref. (*2*), the third column of Table 9 gives the actual (or perturbed) separation of the interacting levels at the crossing point.

The same Coriolis interaction has now been observed to affect levels of $H^{13}C^{14}N$ beginning with the levels $05^{1}0$ and $02^{2}1$. Table 9 shows the perturbations that have been observed for $H^{13}C^{14}N$. In most cases only a single perturbation constant, W_v, could be determined for the coupling between a given pair of states. However, the three resonances observed between the $6\nu_2$ and $3\nu_2 + \nu_3$ states are not fit very well with a single interaction constant, W_v. Instead, we added the *J*-dependent constant, W_{vJ}, given in Eq. [7]. In Table 9 we have given the effective interaction constant at the *J* value for each of the three crossing points.

The interaction constants coupling equivalent states in different isotopomers have similar values, at least in some cases. On the other hand, the constants coupling different vibrational states are often quite different. Some of that difference may be

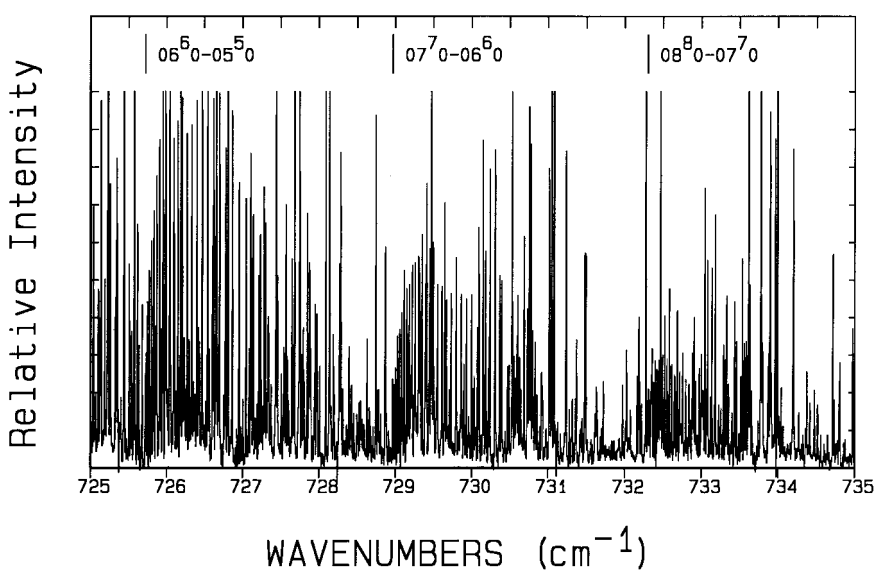

FIG. 3. The emission spectrum of $H^{12}C^{15}N$ showing the region of the $06^{6}0$–$05^{5}0$, $07^{7}0$–$06^{6}0$, and $08^{8}0$–$07^{7}0$ *Q* branches. The first line of each *Q*-branch series is indicated at the top of the plot. The stronger lines have been truncated so that the weaker lines may be seen more easily.

TABLE 5
Rovibrational Constants in cm^{-1} for H^{12}C^{14}N after Correcting for *l*-Type Resonance

v_1 v_2 l v_3	$G_0(v,l)$[a]	B_v	$D_v\times10^6$	$H_v\times10^{12}$	J_{max}
0 0 0 0	0.0	1.478 221 846(22)[b]	2.910 28(14)	3.281(63)	66
0 1 1 0	713.461 342(18)	1.481 772 688(65)	2.977 46(16)	3.914(67)	66
0 2 0 0	1411.413 375(26)	1.485 828 440(104)	3.047 99(20)	5.280(81)	59
0 2 2 0	1432.469 854(23)	1.484 997 246(85)	3.040 79(18)	4.074(73)	60
0 3 1 0	2114.940 064(23)	1.489 575 003(108)	3.113 65(99)	6.047(139)	58
0 3 3 0	2157.151 530(53)	1.487 868 527(227)	3.100 24(108)	3.775(139)	53
0 4 0 0	2802.958 821(38)	1.493 863 846(339)	3.185 74(219)	8.20(26)	53
0 4 2 0	2824.147 481(35)	1.492 984 78(23)	3.174 70(104)	6.17(20)	51
0 4 4 0	2887.627 269(115)	1.490 359 41(67)	3.153 62(223)	2.85(34)	49
0 5 1 0	3496.611 789(73)	1.497 837 57(53)	3.248 66(308)	8.35(45)	53
0 5 3 0	3539.136 736(85)	1.496 029 18(56)	3.231 11(108)	5.62(46)	44
0 5 5 0	3624.011 124(254)	1.492 442 26(136)	3.204 05(397)	3.46(73)	45
0 6 0 0	4174.608 699(218)	1.502 394 81(170)	3.316 4(57)	8.02(180)	42
0 6 2 0	4195.979 257(168)	1.501 468 93(153)	3.311 0(45)	9.94(194)	40
0 6 4 0	4260.002 951(273)	1.498 681 13(160)	3.282 4(25)	5.26(108)	42
0 6 6 0	4366.411 034(388)	1.494 082 98(229)	3.242 2(66)	1.30(167)	39
0 7 1 0	4858.194 777(278)	1.506 643 21(185)	3.375 4(63)	[11.56][c]	43
0 7 3 0	4901.134 999(372)	1.504 738 00(214)	3.388 1(44)	[9.30]	33
0 7 5 0	4986.834 944(353)	1.500 904 44(149)	3.323 99(154)	[4.78]	38
0 7 7 0	5114.926 806(492)	1.495 250 79(196)	3.270 71(856)	[−2.00]	39
0 8 0 0	5525.813 71(54)	1.511 536 40(537)	3.428 7(148)	[13.46]	39
0 8 2 0	5547.421 62(101)	1.510 543 74(562)	3.446 5(121)	[12.33]	33
0 8 4 0	5612.148 81(74)	1.507 580 69(543)	3.442 4(86)	[8.94]	26
0 8 6 0	5719.723 92(113)	1.502 645 15(473)	3.340 8(49)	[3.30]	39
0 8 8 0	5869.649 595(606)	1.495 911 59(264)	3.287 7(117)	[−4.61]	39
0 9 1 0	6198.862 66(71)	1.516 101 44(341)	3.556 7(27)	[14.90]	36
0 9 3 0	[6242.344 29]	[1.514 049 2]	[3.530 0]	[12.64]	
0 9 5 0	6329.079 72(115)	1.509 999 65(820)	3.506 4(124)	[8.12]	25
0 9 7 0	6458.717 10(166)	1.503 925 48(702)	3.310 6(70)	[1.34]	28
0 9 9 0	6630.662 306(700)	1.496 030 90(285)	3.111 68(233)	[−7.70]	35
0 10 0 0	[6855.532 78]	[1.521 366 4]	[3.661]	[17.01]	
0 10 2 0	[6877.425 19]	[1.520 307 8]	[3.636]	[15.88]	
0 10 4 0	[6943.006 15]	[1.517 145 3]	[3.563]	[12.49]	
0 10 6 0	[7051.986 76]	[1.511 919 4]	[3.440]	[6.84]	
0 10 8 0	[7203.884 98]	[1.504 697 8]	[3.269]	[−1.07]	
0 10 10 0	7398.036 51(136)	1.495 555 7(163)	3.260 4(457)	[−11.23]	21
0 0 0 1	2096.845 558(27)	1.468 142 050(133)	2.916 20(28)	3.21(14)	48
0 1 1 1	2807.053 505(47)	1.471 573 85(29)	2.982 54(45)	3.92(19)	48
0 2 0 1	3502.119 692(61)	1.475 493 33(44)	3.050 17(75)	5.40(42)	46
0 2 2 1	3522.770 241(59)	1.474 677 90(41)	3.045 20(69)	4.50(31)	45
0 3 1 1	4202.684 614(49)	1.479 106 85(54)	3.110 7(18)	5.30(108)	40
0 3 3 1	4244.133 873(155)	1.477 426 82(109)	3.103 9(23)	4.60(104)	41
0 4 0 1	4888.039 045(299)	1.483 252 97(232)	3.180 6(56)	[7.57]	38
0 4 2 1	4908.867 504(418)	1.482 383 29(197)	3.167 8(31)	[6.44]	35
0 4 4 1	4971.276 904(420)	1.479 788 14(191)	3.152 6(28)	[3.06]	37
0 5 1 1	5578.931 552(361)	1.487 110 50(356)	3.289 9(68)	[8.61]	32
0 5 3 1	5620.780 89(169)	1.485 302 9(108)	3.210 8(148)	[6.35]	26
0 5 5 1	5704.316 32(99)	1.481 744 95(354)	3.195 0(57)	[1.84]	36
0 6 0 1	[6254.378 32]	[1.491 538 8]	[3.346]	[10.32]	
0 6 2 1	[6275.435 37]	[1.490 609 4]	[3.330]	[9.19]	
0 6 4 1	[6338.531 25]	[1.487 834 5]	[3.285]	[5.80]	
0 6 6 1	6443.390 24(147)	1.483 240 13(523)	3.229 5(76)	[0.15]	34

[a] To get observed band center use $G_c(v,l) = G_0(v,l) - B_v l^2 - D_v l^4 - H_v l^6$.
[b] The uncertainty in the last digits, twice the estimated standard error, is given in parentheses.
[c] Constants enclosed in square brackets were fixed for the least-squares fit.

a normal vibrational dependence, but other factors may be involved.

Vibrational Resonances

There is another accidental crossing of energy levels that occurs in both H^{12}C^{14}N and H^{13}C^{14}N. In the former case the $02^{2e}2$ level is crossed by the $08^{2e}0$ level at $J = 28$ and in the latter case the $02^{0}2$ and $08^{0}0$ levels cross as well as the $02^{2}2$ and $08^{2}0$ levels. This latter case will be discussed first.

According to the constants given in Table 10, the $02^{0}2$ vibrational level for H^{13}C^{14}N is only about 6.7 cm^{-1} above the $08^{0}0$ level. The lower level has a larger B-value and so must overtake and cross the $02^{0}2$ level between $J = 12$ and $J = 14$. In fact we estimate that the $J = 13$ levels are only about 0.01 ± 0.10 cm^{-1} apart. Since the two levels have the same symmetry, a vibrational resonance between them is possible with a direct resonance constant due to the $k_{22222233}$ term in the potential function. Other scenarios for the perturbation could

TABLE 6
Rovibrational Constants in cm^{-1} for $H^{12}C^{15}N$ after Correcting for *l*-Type Resonance

$v_1v_2l\,v_3$	$G_0(v,l)$[a]	B_v	$D_v\times10^6$	$H_v\times10^{12}$	J_{max}
0 0 0 0	0.0	1.435 247 967(72)[b]	2.746 58(20)	2.864(64)	65
0 1 1 0	712.465 207(23)	1.438 653 049(42)	2.808 74(19)	3.407(64)	65
0 2 0 0	1409.306 512(37)	1.442 537 901(57)	2.873 77(21)	4.592(72)	61
0 2 2 0	1430.526 036(35)	1.441 746 413(85)	2.867 61(21)	3.558(69)	66
0 3 1 0	2111.776 619(35)	1.446 127 174(95)	2.934 43(53)	5.251(76)	60
0 3 3 0	2154.309 033(60)	1.444 502 562(134)	2.922 96(54)	3.262(76)	66
0 4 0 0	2798.635 100(66)	1.450 231 738(434)	3.000 12(113)	6.662(183)	57
0 4 2 0	2819.981 737(60)	1.449 395 644(279)	2.991 86(59)	5.602(125)	54
0 4 4 0	2883.935 058(127)	1.446 895 57(49)	2.972 74(112)	2.433(178)	52
0 5 1 0	3491.186 843(88)	1.454 036 307(352)	3.059 57(142)	[7.547][c]	56
0 5 3 0	3534.023 023(121)	1.452 315 961(611)	3.045 87(83)	5.444(313)	45
0 5 5 0	3619.518 665(189)	1.448 898 64(72)	3.018 80(186)	2.174(231)	52
0 6 0 0	4167.987 14(23)	1.458 401 82(169)	3.131 59(367)	10.44(155)	51
0 6 2 0	4189.512 107(187)	1.457 509 73(120)	3.114 13(252)	7.33(89)	46
0 6 4 0	4253.995 814(211)	1.454 858 61(116)	3.092 84(173)	5.33(75)	45
0 6 6 0	4361.167 708(213)	1.450 480 47(85)	3.055 33(290)	0.48(40)	49
0 7 1 0	4850.441 164(255)	1.462 458 16(133)	3.188 76(292)	[10.20]	49
0 7 3 0	4893.687 122(365)	1.460 620 75(168)	3.158 58(235)	[8.23]	34
0 7 5 0	4979.988 927(258)	1.456 994 17(99)	3.132 87(89)	[4.28]	41
0 7 7 0	5108.982 072(250)	1.451 611 90(77)	3.084 11(41)	[−1.65]	48
0 8 0 0	5516.842 174(873)	1.467 149 0(86)	3.209 1(143)	[11.93]	35
0 8 2 0	[5538.601 76]	[1.466 173 9]	[3.240]	[10.94]	
0 8 4 0	5603.778 407(593)	1.463 347 0(30)	3.205 1(46)	[7.97]	33
0 8 6 0	5712.083 576(409)	1.458 690 56(178)	3.166 2(23)	[3.03]	35
0 8 8 0	5863.053 128(318)	1.452 260 35(107)	3.104 9(55)	[−3.89]	39
0 9 1 0	[6188.754 85]	[1.471 471 6]	[3.304]	[13.25]	
0 9 3 0	[6232.516 28]	[1.469 521 8]	[3.284]	[11.27]	
0 9 5 0	6319.847 21(88)	1.465 654 7(54)	3.237 1(69)	[7.32]	28
0 9 7 0	6450.353 988(554)	1.459 908 56(273)	3.181 9(34)	[1.39]	32
0 9 9 0	6623.463 112(473)	1.452 391 01(170)	3.110 3(74)	[−6.51]	37
0 10 0 0	[6844.150 66]	[1.476 486 2]	[3.367]	[15.17]	
0 10 2 0	[6866.194 08]	[1.475 477 7]	[3.356]	[14.18]	
0 10 4 0	[6932.225 31]	[1.472 466 0]	[3.325]	[11.21]	
0 10 6 0	[7041.947 20]	[1.467 492 5]	[3.274]	[6.27]	
0 10 8 0	7194.864 13(91)	1.460 609 3(68)	3.180 2(116)	[−0.64]	25
0 10 10 0	7390.284 05(78)	1.451 967 5(42)	3.107 0(105)	[−9.54]	31
0 11 1 0	[7504.789 89]	[1.481 183 7]	[3.431]	[16.69]	
0 11 3 0	[7549.181 42]	[1.479 103 7]	[3.408]	[14.71]	
0 11 5 0	[7637.762 04]	[1.474 971 2]	[3.362]	[10.76]	
0 11 7 0	[7770.126 89]	[1.468 841 5]	[3.294]	[4.83]	
0 11 9 0	[7945.668 49]	[1.460 797 4]	[3.203]	[−3.08]	
0 11 11 0	8163.576 12(126)	1.450 949 8(74)	3.085 7(150)	[−12.96]	28
0 0 0 1	2064.316 161(47)	1.425 579 234(136)	2.752 038(343)	2.88(17)	50
0 1 1 1	2773.650 840(48)	1.428 870 742(345)	2.812 658(589)	3.32(23)	49
0 2 0 1	3467.783 161(79)	1.432 618 969(839)	2.875 94(183)	5.54(107)	47
0 2 2 1	3488.538 125(96)	1.431 850 163(642)	2.871 064(1024)	4.12(41)	45
0 3 1 1	4167.450 681(97)	1.436 077 73(72)	2.930 48(145)	4.52(70)	48
0 3 3 1	4209.117 017(188)	1.434 495 40(139)	2.930 55(258)	6.50(124)	41
0 4 0 1	4851.834 707(166)	1.440 041 80(167)	2.993 6(35)	9.24(202)	38
0 4 2 1	4872.774 810(166)	1.439 222 46(135)	2.988 5(25)	6.98(105)	43
0 4 4 1	4935.520 086(457)	1.436 769 62(222)	2.975 8(24)	[2.66]	31
0 5 1 1	[5541.781 17]	[1.443 713 8]	[3.052]	[7.55]	
0 5 3 1	[5583.870 51]	[1.442 019 3]	[3.043]	[5.57]	
0 5 5 1	[5667.872 81]	[1.438 658 5]	[3.025]	[1.62]	

[a] To get observed band center use $G_c(v,l) = G_0(v,l) - B_v l^2 - D_v l^4 - H_v l^6$.
[b] The uncertainty in the last digits, twice the estimated standard deviation, is given in parentheses.
[c] The values enclosed in square brackets were fixed in the least-squares fit.

be found involving more indirect perturbations operating through larger potential constants but between more distant levels.

We have only one measurement of the $J = 13$ level for 08^00 and it does not seem to be displaced from its expected position, nor do the adjoining rotational levels. It can also be shown that the 02^22 levels are crossed by the 08^20 levels with the $J = 10$ level of $02^{2e}2$ being 0.27 ± 0.15 cm^{-1} above that of the $08^{2e}0$ level and the $J = 11$ level of $02^{2f}2$ being 0.21 ± 0.15 cm^{-1} below that of $08^{2f}0$, although none of these levels have been observed. Other levels are expected to be more distant.

The crossing of the $02^{2e}2$ and $08^{2e}0$ levels of $H^{12}C^{14}N$ also seems not to result in any perturbation of the levels. We have tried to use a vibrational perturbation matrix element in the analysis of the measurements for those two states and the constant cannot be determined, but it must be small. In this case, however, the relevant levels of the two states are always

TABLE 7

Rovibrational Constants in cm^{-1} for $H^{13}C^{14}N$ after Correcting for *l*-Type Resonance

v_1	v_2	l	v_3	$G_0(v,l)$[a]	B_v	$D_v \times 10^6$	$H_v \times 10^{12}$	J_{max}
0	0	0	0	0.0	1.440 000 472(69)[b]	2.768 54(18)	2.701(58)	69
0	1	1	0	707.408 891(21)	1.443 157 181(56)	2.827 74(19)	3.215(62)	69
0	2	0	0	1399.760 658(34)	1.446 801 862(133)	2.889 54(24)	4.344(76)	59
0	2	2	0	1420.418 451(31)	1.445 995 548(93)	2.883 41(21)	3.336(71)	61
0	3	1	0	2097.719 897(27)	1.450 144 159(132)	2.947 81(114)	4.62(14)	55
0	3	3	0	2139.156 364(83)	1.448 490 235(260)	2.934 19(125)	3.14(11)	56
0	4	0	0	2780.585 370(52)	1.454 009 157(302)	3.009 68(241)	[5.73][c]	54
0	4	2	0	2801.396 409(51)	1.453 158 84(31)	3.002 23(126)	4.94(18)	52
0	4	4	0	2863.745 264(148)	1.450 615 79(55)	2.979 35(256)	2.47(18)	54
0	5	1	0	3469.106 005(109)	1.457 566 02(51)	3.066 37(334)	[6.28]	50
0	5	3	0	3510.895 190(130)	1.455 818 26(54)	3.051 37(106)	[4.65]	47
0	5	5	0	3594.301 517(191)	1.452 344 23(61)	3.017 48(450)	[1.39]	51
0	6	0	0	4142.356 311(238)	1.461 688 66(145)	3.129 4(50)	[7.24]	46
0	6	2	0	4163.368 023(274)	1.460 789 15(112)	3.119 3(41)	[6.43]	44
0	6	4	0	4226.315 447(266)	1.458 095 20(105)	3.093 18(82)	[3.98]	38
0	6	6	0	4330.934 569(263)	1.453 648 58(88)	3.048 16(682)	[-0.10]	44
0	7	1	0	4821.211 305(591)	1.465 508 80(331)	3.186 1(79)	[7.79]	43
0	7	3	0	4863.452 294(480)	1.463 643 40(261)	3.161 0(52)	[6.16]	37
0	7	5	0	4947.749 918(494)	1.459 960 02(200)	3.129 7(23)	[2.90]	38
0	7	7	0	5073.746 837(376)	1.454 498 75(143)	3.071 2(98)	[-1.99]	44
0	8	0	0	5484.466 98(76)	1.469 945 81(559)	3.238 3(120)	[8.75]	23
0	8	2	0	[5505.732 40]	[1.468 967 1]	[3.24]	[7.94]	
0	8	4	0	5569.432 19(91)	1.466 108 67(629)	3.205 4(103)	[5.49]	25
0	8	6	0	5675.284 71(70)	1.461 376 01(345)	3.152 4(50)	[1.41]	29
0	8	8	0	5822.832 383(513)	1.454 862 63(180)	3.083 4(137)	[-4.30]	44
0	9	1	0	[6153.178 57]	[1.474 033 6]	[3.308]	[9.30]	
0	9	3	0	[6195.973 33]	[1.472 060 2]	[3.285]	[7.67]	
0	9	5	0	[6281.372 82]	[1.468 140 3]	[3.239]	[4.41]	
0	9	7	0	6408.996 77(118)	1.462 315 63(822)	3.171 2(140)	[-0.48]	25
0	9	9	0	6578.276 088(726)	1.454 704 13(310)	3.082 1(178)	[-7.01]	33
0	10	0	0	[6805.804 85]	[1.478 813 1]	[3.370]	[10.26]	
0	10	2	0	[6827.373 26]	[1.477 793 4]	[3.358]	[9.45]	
0	10	4	0	[6891.981 24]	[1.474 747 6]	[3.321]	[7.00]	
0	10	6	0	[6999.337 02]	[1.469 716 0]	[3.260]	[2.92]	
0	10	8	0	7148.955 33(136)	1.462 731 6(101)	3.168 9(172)	[-2.79]	26
0	10	10	0	7340.152 63(92)	1.453 989 30(424)	3.067 9(226)	[-10.13]	32
0	11	1	0	[7463.620 43]	[1.483 273 3]	[3.426]	[10.81]	
0	11	3	0	[7507.078 50]	[1.481 171 8]	[3.401]	[9.18]	
0	11	5	0	[7593.795 64]	[1.476 995 6]	[3.349]	[5.92]	
0	11	7	0	[7723.373 86]	[1.470 798 4]	[3.271]	[1.02]	
0	11	9	0	[7895.216 16]	[1.462 661 0]	[3.168]	[-5.50]	
0	11	11	0	8108.525 63(124)	1.452 687 0(78)	3.053 9(296)	[-13.66]	27
0	0	0	1	2063.047 099(46)	1.430 246 801(292)	2.774 99(54)	3.03(27)	50
0	1	1	1	2766.737 760(75)	1.433 299 14(38)	2.833 15(60)	3.52(27)	50
0	2	0	1	3455.790 658(78)	1.436 823 43(58)	2.893 74(67)	[4.22]	46
0	2	2	1	3476.021 425(94)	1.436 032 78(44)	2.886 95(37)	[3.41]	43
0	3	1	1	4150.400 239(154)	1.440 047 05(110)	2.947 9(20)	5.27(60)	47
0	3	3	1	4191.035 625(308)	1.438 422 42(131)	2.938 4(17)	[3.14]	42
0	4	0	1	4830.254 576(507)	1.443 790 97(433)	3.015 0(116)	[5.73]	37
0	4	2	1	4850.688 54(54)	1.442 944 30(252)	2.999 3(43)	[4.92]	36
0	4	4	1	4911.913 19(54)	1.440 436 74(260)	2.978 9(35)	[2.47]	36
0	5	1	1	[5515.679 27]	[1.447 228 6]	[3.068]	[6.28]	
0	5	3	1	5556.773 20(198)	1.445 473 4(119)	3.020 2(163)	[4.65]	24
0	5	5	1	5638.779 00(87)	1.442 049 04(480)	3.007 6(73)	[1.39]	28
0	0	0	2	4105.874 995(627)	1.420 442 0(66)	2.786 2(110)	[3.25]	25
0	1	1	2	4805.601 14(28)	1.423 389 89(424)	2.845 4(105)	[3.66]	21
1	0	0	0	3293.513 232(117)	1.430 372 61(64)	2.746 80(88)	3.38(33)	46
1	1	1	0	3982.205 909(66)	1.433 718 62(22)	2.809 27(15)	[3.56]	42
1	2	0	0	4655.840 604(168)	1.437 567 61(127)	2.878 77(139)	[4.69]	33
1	2	2	0	4676.255 877(165)	1.436 748 13(94)	2.870 58(98)	[4.09]	32
1	3	1	0	5334.865 200(319)	1.441 113 3(35)	2.944 5(68)	[5.21]	24
1	3	3	0	5375.770 191(531)	1.439 426 8(64)	2.911 6(140)	[4.00]	21
2	0	0	0	6483.281 24(21)	1.420 456 62(101)	2.725 47(89)	[4.02]	35
2	1	1	0	7153.082 61(22)	1.423 989 43(161)	2.792 5(216)	[4.54]	29
2	2	0	0	7807.962 196(891)	1.428 028 2(168)	2.884 7(858)	[5.36]	16
2	2	2	0	7827.985 52(117)	1.427 199 1(237)	2.826(110)	[4.76]	18
1	0	0	1	5343.658 669(156)	1.420 812 00(87)	2.756 66(89)	[3.58]	33
1	1	1	1	6028.769 89(21)	1.424 068 68(238)	2.823 0(51)	[4.10]	24
1	2	0	1	6699.101 06(42)	1.427 826 6(73)	[2.885]	[4.92]	20
1	2	2	1	[6719.318 18]	[1.427 004 8]	[2.875]	[4.32]	
2	0	0	1	8519.244 37(100)	1.411 077 3(166)	2.708 7(521)	[4.25]	18
3	0	0	0	9571.696 401(568)	1.410 231 8(69)	2.693 9(157)	[4.69]	22

[a] To get observed band center use $G_c(v,l) = G_0(v,l) - B_v l^2 - D_v l^4 - H_v l^6$.

[b] The uncertainty in the last digits, twice the estimated standard error, is given in parentheses.

[c] Constants enclosed in square brackets were fixed for the least-squares fit.

TABLE 8
***l*-Type Resonance Constants in cm^{-1} for $H^{12}C^{14}N$, $H^{12}C^{15}N$, and $H^{13}C^{14}N$**

$v_1v_2v_3$	$q_v\times10^3$	$q_{vJ}\times10^8$	$q_{vJJ}\times10^{12}$	$\rho_v\times10^8$
$H^{12}C^{14}N$				
0 1 0	7.487 737 5(17)[a]	8.874 9(18)	1.362(12)	
0 2 0	7.595 614(664)	9.319 0(77)	1.408(25)[b]	[-1.84][c]
0 3 0	7.709 264(38)	9.878 7(99)	1.581(55)	-1.964(73)
0 4 0	7.824 983(171)	10.427 6(243)	1.767(98)	-2.007(73)
0 5 0	7.946 026(148)	11.020 5(304)	1.660(140)	-2.123(74)
0 6 0	8.070 21(29)	11.610(29)	[1.78]	-2.164(72)
0 7 0	8.200 98(35)	12.186(52)	[1.86]	-2.284(74)
0 8 0	8.339 18(247)	13.263(293)	[1.95]	-2.613(183)
0 9 0	8.476 41(51)	[13.65]	[2.03]	[-2.37]
0 10 0	[8.623 0]	[14.40]	[2.12]	[-2.45]
0 1 1	7.479 547(393)	8.762 0(636)	1.07(24)	
0 2 1	7.573 41(78)	9.167(46)	[1.44]	[-1.79]
0 3 1	7.673 968(309)	9.620(96)	1.41(72)	-1.917(77)
0 4 1	7.778 25(201)	10.106(122)	[1.61]	-1.850(181)
0 5 1	7.896 22(130)	12.420(214)	[1.69]	[-2.00]
0 6 1	[7.995 2]	[10.99]	[1.78]	[-2.10]
$H^{12}C^{15}N$				
0 1 0	7.069 679 0(29)	8.091 7(37)	1.190(14)	
0 2 0	7.171 19(37)	8.531 4(172)	1.305(38)[b]	[-1.700]
0 3 0	7.277 459(73)	9.017 6(90)	1.455(25)	-1.800(34)
0 4 0	7.385 494(166)	9.481(20)	1.499(62)	-1.831(34)
0 5 0	7.498 983(135)	10.019 4(177)	1.531(57)	-1.941(34)
0 6 0	7.617 30(35)	10.707(66)	1.92(35)	-1.979(34)
0 7 0	7.740 92(32)	11.299(49)	1.94(12)	-2.122(35)
0 8 0	7.874 0(36)	[11.90]	[1.99]	[-2.18]
0 9 0	[8.001 1]	[12.58]	[2.10]	[-2.26]
0 10 0	[8.140 5]	[13.30]	[2.21]	[-2.34]
0 11 0	[8.286 4]	[14.06]	[2.33]	[-2.42]
0 1 1	7.064 002(378)	8.031 4(713)	1.225(274)	
0 2 1	7.147 68(100)	8.332(164)	1.80(83)	[-1.645]
0 3 1	7.239 552(382)	8.720(80)	1.26(41)	-1.712(41)
0 4 1	7.331 70(74)	9.131(63)	[1.54]	[-1.80]
0 5 1	[7.429 3]	[9.54]	[1.66]	[-1.88]
$H^{13}C^{14}N$				
0 1 0	7.166 195(13)	8.107 3(58)	1.135(18)	
0 2 0	7.268 75(80)	8.495 1(186)	1.159(41)[b]	[-1.714]
0 3 0	7.375 054(91)	8.969 1(171)	1.099(74)	-1.752(82)
0 4 0	7.483 926(198)	9.430 7(235)	1.136(76)	-1.805(80)
0 5 0	7.598 273(210)	9.991(30)	1.20(11)	-1.885(82)
0 6 0	7.714 28(46)	10.357(63)	0.45(20)	-1.926(81)
0 7 0	7.838 21(68)	10.998(156)	1.07(37)	-1.921(91)
0 8 0	[7.965 1]	[11.61]	[1.1]	[-2.004]
0 9 0	[8.098 1]	[12.22]	[1.1]	[-2.05]
0 10 0	[8.237 0]	[12.87]	[1.1]	[-2.10]
0 11 0	[8.382 3]	[13.54]	[1.1]	[-2.14]
0 1 1	7.151 280(430)	8.050 7(738)	1.07(27)	
0 2 1	7.238 63(99)	8.453(64)	[1.1]	[-1.579]
0 3 1	7.331 685(584)	8.638(91)	[1.1]	-1.618(96)
0 4 1	7.432 75(291)	9.505(239)	[1.1]	-1.774(272)
0 5 1	[7.526 4]	[9.441]	[1.1]	[-1.726]
1 1 0	7.291 540(234)	8.723(19)	[1.1]	
1 2 0	7.404 91(173)	9.252(170)	[1.1]	[-1.714]
1 3 0	7.525 92(237)	10.47(58)	[1.1]	[-1.752]
1 1 1	7.355 49(287)	9.63(78)	[1.1]	
1 2 1	7.494 3(233)	[9.55]	[1.1]	[-1.714]
2 1 0	7.378 60(206)	8.556(339)	[1.1]	
2 2 0	7.478 0(558)	[9.86]	[1.1]	[-1.714]
0 1 2	7.136 69(208)	[8.10]	[1.1]	

[a] The uncertainty in the last digits, twice the estimated standard error, is given in parentheses.
[b] For $v_2 > 1$ the data were fit with $q_l(H^{12}C^{14}N) = (0.828\pm0.033)\times10^{-5}$ cm^{-1}, $q_l(H^{12}C^{15}N) = (0.854\pm0.017)\times10^{-5}$ cm^{-1}, and $q_l(H^{13}C^{14}N) = (0.705\pm0.038)\times10^{-5}$ cm^{-1}.
[c] Values enclosed in square brackets were fixed for the least-squares fit.

separated by more than 0.9 cm^{-1}, so a weak interaction would be difficult to detect.

These measurements indicate that these vibrational perturbations are too weak to displace the levels by more than 0.0005 cm^{-1}. That is not surprising because such a high-order potential constant should be quite small and any indirect resonance mechanism also would be expected to have a small effect. It does show, however, that the normal rules for interactions still seem to be effective as we go higher in the potential function. In a collision-free environment there is very little mixing of the high bending states with nearby states containing some degree of stretching motion, even when they have the same symmetry.

VIBRATIONAL DEPENDENCE OF THE CONSTANTS

To extend our ability to calculate term values for higher bending states, we have included the present measurements in a new least-squares fit of the various constants given in Tables 5–8 to determine the best constants for the usual power series expansion in the vibrational quantum numbers and the quantum number for vibrational angular momentum, l. The vibrational term values were fit to the equation:

$$\begin{aligned} G_0(v, l) + G(0, 0) &= \sum \omega_i(v_i + d_i/2) + \sum\sum x_{ij}(v_i + d_i/2)(v_j + d_j/2) \\ &\quad + g_{22}l^2 + \sum\sum\sum y_{ijk}(v_i + d_i/2)(v_j + d_j/2) \\ &\quad \times (v_k + d_k/2) + \sum y_{ill}(v_i + d_i/2)l^2 \\ &\quad + \sum\sum\sum\sum z_{ijkh}(v_i + d_i/2)(v_j + d_j/2)(v_k + d_k/2) \\ &\quad \times (v_h + d_h/2) + \cdots. \end{aligned} \quad [8]$$

TABLE 9
New Coriolis Interactions Found for $H^{12}C^{14}N$, $H^{13}C^{14}N$, and $H^{12}C^{15}N$

states involved	J at avoided-crossing	separation at avoided-crossing (cm^{-1})	uppermost level at crossing	interaction constant, W_v[a] (cm^{-1})
$H^{12}C^{14}N$				
08^60-05^51	8	0.1341	05^51	0.004738(43)
$08^{2e}0$-$05^{1e}1$	26	0.4801	$05^{1e}1$	0.004738(43)
09^70-06^61	15	0.3921	09^70	0.014435(45)
$H^{13}C^{14}N$				
$13^{1e}0$-10^01	29	0.0676	10^01	ND[b]
$08^{2e}0$-$05^{3e}1$	36	0.4121	$08^{2e}0$	ND
$07^{3e}0$-$04^{4e}1$	43	0.6306	$07^{3e}0$	[0.001767]
$07^{3f}0$-$04^{4f}1$	35	0.5658	$04^{4f}1$	[0.001767]
$07^{1f}0$-$04^{2f}1$	28	0.3653	$04^{2f}1$	0.001767(11)
$07^{1e}0$-04^01	33	0.2669	04^01	0.001767(11)
$06^{2e}0$-$03^{3e}1$	26	0.7756	$06^{2e}0$	0.002433[c]
$06^{2f}0$-$03^{3f}1$	36	0.1949	$06^{2f}0$	0.002648
06^00-$03^{1e}1$	16	0.2753	$03^{1e}1$	0.002287
$05^{1e}0$-$02^{2e}1$	18	0.0817	$05^{1e}0$	0.002480(11)
$05^{1f}0$-$02^{2f}1$	8	0.2823	$02^{2f}1$	[0.002480]
$H^{12}C^{15}N$				
08^00-$05^{1e}1$	39	0.8135	08^00	ND
$08^{2e}0$-$05^{1e}1$	13	0.3673	$05^{1e}1$	ND
$08^{2f}0$-$05^{1f}1$	26	0.3327	$05^{1f}1$	ND

[a] The uncertainties given in this table are twice the standard deviation.
[b] ND indicates that the constant was not determined.
[c] The three avoided crossings for $v_2 = 6$ were fit to the constants $W_v = 0.002\,194 \pm 0.000\,027$ cm^{-1} and $W_{vJ} = 0.34 \pm 0.03 \times 10^{-6}$ cm^{-1}, see text.

TABLE 10
Constants in cm^{-1} for the Vibrational Energy Levels of Four Isotopomers of HCN

Parameter	$H^{12}C^{14}N$	$H^{13}C^{14}N$	$H^{12}C^{15}N$	$H^{13}C^{15}N$
ω_1	3443.092 07(3226)[a]	3424.006 90(2999)	3441.700 57(2089)	3422.579 10(1779)
ω_2	726.959 68(575)	720.572 67(704)	725.905 83(660)	719.501 22(530)
ω_3	2127.397 48(4842)	2092.985 12(2164)	2093.952 08(2968)	2058.636 00(446)
x_{11}	−53.222 286(10616)	−53.336 468(22226)	−53.310 336(7857)	−53.292 10(844)
x_{22}	−2.596 975(2083)	−2.458 978(759)	−2.620 141(2149)	−2.486 960(2156)
x_{33}	−10.080 943(37673)	−9.897 972(5935)	−9.784 584(14869)	[−9.6][b]
x_{12}	−18.954 192(9784)	−18.365 549(21105)	−18.913 788(9840)	−18.270 02(659)
x_{13}	−13.875 846(83596)	−12.530 413(55348)	−13.564 265(44166)	−11.988 53(643)
x_{23}	−3.206 376(8665)	−3.705 772(1442)	−3.061 520(11203)	−3.578 05(494)
g_{22}	5.314 581(1065)	5.209 069(440)	5.364 149(1586)	5.251 667(1017)
y_{111}	0.452 390(2733)	0.401 051(7579)	0.417 447(1495)	[0.37]
y_{222}	0.020 448(450)	0.017 109(128)	0.021 534(356)	0.019 300(331)
y_{333}	−0.038 823(11160)	[−0.039]	[−0.038]	[−0.039]
y_{112}	−0.105 669(3635)	−0.056 99(1626)	−0.080 723(1121)	[−0.083]
y_{122}	−0.075 275(1820)	−0.094 189(1331)	−0.089 721(3739)	−0.107 528(2328)
y_{113}	−0.457 134(10767)	−0.211 58(3002)	−0.355 457(2902)	[−0.29]
y_{133}	0.118 946(54287)	0.139 35(1169)	0.147 340(22248)	[0.158]
y_{123}	0.102 603(15159)	0.009 352(367)	−0.003 220(3412)	−0.099 993(5859)
y_{233}	−0.122 485(4610)	−0.113 005(513)	−0.122 240(5439)	[−0.111]
y_{223}	0.090 497(723)	0.115 073(332)	0.109 095(643)	0.143 419(1424)
y_{1ll}	−0.036 003(1162)	−0.034 356(903)	−0.029 157(3042)	−0.012 728(977)
y_{2ll}	0.004 421(413)	0.007 815(108)	0.003 605(309)	0.007 005(297)
y_{3ll}	−0.122 773(981)	−0.140 156(297)	−0.153 534(2395)	−0.166 449(901)
z_{1111}	0.009 434 4(2210)	0.011 166(1136)	[0.009 4]	[0.009 67]
z_{2222}	−0.001 153 6(481)	−0.001 063 5(130)	−0.001 201 2(287)	−0.001 217 9(149)
z_{3333}	0.005 404 1(13756)	[0.005 3]	[0.005 3]	[0.005 8]
z_{1112}	−0.018 369 9(5415)	−0.022 821(3595)	[−0.018]	[−0.017 5]
z_{1113}	−0.123 247 9(18075)	−0.137 670(6657)	[−0.121]	[−0.121]
z_{1122}	0.013 781 3(3318)	0.015 604(362)	[0.013 7]	[0.015 5]
z_{1133}	0.055 282 2(48422)	[0.051 4]	[0.055]	[0.051 4]
z_{1123}	0.088 754 4(16319)	[0.088]	[0.088 5]	[0.093 5]
z_{1222}	0.001 647 0(1808)	0.002 394 5(1249)	0.002 990 8(5013)	0.003 456 1(2944)
z_{1333}	−0.028 285 5(78050)	[−0.028 0]	[−0.028]	[−0.033 6]
z_{1223}	−0.013 397 9(6744)	[−0.013 3]	[−0.013]	[−0.013 3]
z_{1233}	−0.033 945 4(66859)	[−0.033 0]	[−0.033 5]	[−0.036 6]
z_{2223}	−0.004 050 0(605)	−0.004 783 6(413)	−0.005 482 7(731)	−0.006 901 9(1612)
z_{2233}	0.008 487 6(2014)	[0.008 26]	[0.008 5]	[0.008 26]
z_{2333}	−0.002 680 1(6978)	[−0.002 5]	[−0.002 5]	[−0.002 5]
z_{11ll}	−0.015 617 9(2379)	−0.018 683 0(2858)	[−0.015 5]	[−0.018 7]
z_{22ll}	0.001 382 5(654)	0.001 299 2(133)	0.001 431 4(304)	0.001 420 9(173)
z_{33ll}	−0.007 157 0(2467)	[−0.007 3]	[−0.007 1]	[−0.007 3]
z_{12ll}	−0.005 114 1(2119)	−0.005 830 2(1498)	−0.006 963(493)	−0.007 637 9(2599)
z_{13ll}	0.036 093 3(8474)	0.057 184 9(5074)	0.058 022 2(47306)	[0.057 4]
z_{23ll}	0.005 910 7(1029)	0.006 480 1(310)	0.007 563 8(813)	0.008 567 2(2450)
z_{llll}	−0.000 388 03(1604)	−0.000 377 41(298)	−0.000 389 5(68)	−0.000 465 19(692)
z_{2lll}	−0.000 011 42(202)	−0.000 011 77(36)	−0.000 011 54(83)	
z_{222ll}	0.000 013 69(389)	0.000 013 39(87)	0.000 011 40(196)	
z_{22222}	−0.000 008 08(208)	−0.000 008 014(623)	−0.000 006 08(136)	
std. dev. of fit	17.4	2.9	7.2	14.0
Number of non-zero weighted measurements:				
	129	73	62	27

[a] The uncertainty (one standard deviation) in the last digits is given in parentheses.
[b] Values enclosed in square brackets were fixed during the fit.

Here since we have defined $G_0(0, 0)$ equal to zero, then $G(0, 0)$ represents the zero-point vibrational energy. In this and the following equations the sums are over all values of the subscript from 1 to 3 except that $h \geq k \geq j \geq i$ and the degeneracy is given by $d_1 = d_3 = 1$ and $d_2 = 2$. These constants are given in Table 10. In Tables 10–13 we also give constants for $H^{13}C^{15}N$ based on some preliminary measurements. A more complete summary of data for $H^{13}C^{15}N$ based on both absorption and emission spectra will be published when the analysis of the emission spectrum is completed.

The usual expression for the rotational constants was used to determine the constants given in Table 11:

TABLE 11
Rotational Constants in $cm^{-1} \times 10^{-3}$ for Four Isotopomers of HCN

Parameter	$H^{12}C^{14}N$	$H^{13}C^{14}N$	$H^{12}C^{15}N$	$H^{13}C^{15}N$
B_e	1484.775 403(1981)	1446.386 010(3430)[a]	1441.534 949(6771)	1402.551 283(3485)
α_1	10.429 87(365)	9.612 87(686)	10.009 02(319)	9.211 56(615)
α_2	−3.570 53(215)	−3.182 40(181)	−3.423 32(161)	−3.037 34(358)
α_3	10.005 42(259)	9.688 31(546)	9.591 86(1756)	9.268 82(628)
γ_{11}	−0.146 922(1875)	−0.138 874(3810)	−0.144 308(763)	−0.137 076(781)
γ_{22}	0.046 480(908)	0.043 785(518)	0.042 917(469)	0.043 290(940)
γ_{33}	−0.029 213(328)	−0.026 134(2465)	−0.031 328(8759)	[−0.028][b]
γ_{12}	0.194 157(1125)	0.168 658(2855)	0.191 289(1914)	0.170 942(5689)
γ_{13}	0.193 750(3530)	0.166 865(3773)	0.186 503(1793)	0.158 034(11409)
γ_{23}	−0.114 872(2963)	−0.100 423(1924)	−0.108 049(1855)	−0.098 225(6525)
γ_{ll}	−0.195 086(633)	−0.189 172(319)	−0.185 688(591)	−0.181 847(522)
γ_{111}	−0.001 323 0(3205)	−0.001 718(771)	[−0.001 3]	[−0.001 5]
γ_{222}	0.000 341 9(1358)	0.000 362 4(799)	0.000 550 4(691)	0.000 135 3(1598)
γ_{333}	[0.0]	[0.0]	[0.0]	[0.0]
γ_{112}	[0.0]	[0.0]	[0.0]	[0.0]
γ_{113}	0.002 789 5(11604)	[0.002 5]	[0.002 5]	[0.002 5]
γ_{122}	0.003 529 2(2318)	0.004 341 5(5588)	0.004 186 9(4357)	0.003 278 6(2097)
γ_{223}	−0.006 997 4(12356)	−0.007 543 0(2304)	−0.008 091 1(3588)	−0.009 735(1255)
γ_{133}	[0.0]	[0.0]	[0.0]	[0.0]
γ_{233}	[0.0]	[0.0]	[0.0]	[0.0]
γ_{123}	0.015 579 8(8297)	0.020 281(2987)	[0.015]	0.028 72(1115)
γ_{1ll}	−0.002 892 2(9347)	−0.003 558 4(4804)	−0.004 660 0(2854)	−0.005 219(112)
γ_{2ll}	−0.004 059 2(1315)	−0.003 901 7(632)	−0.003 941 1(1398)	−0.003 186(170)
γ_{3ll}	0.008 317 0(8158)	0.008 105 5(1586)	0.010 252(1091)	0.013 752(801)
γ_{2222}	0.000 056 02(602)	0.000 045 76(559)	0.000 034 52(474)	0.000 054 71(960)
γ_{2223}	0.000 561 3(1565)	[0.000 60]	[0.000 6]	0.000 758 4(1511)
γ_{11ll}	0.001 072(282)	[0.001 00]	[0.001 0]	[0.001 0]
γ_{22ll}	−0.000 192 40(929)	−0.000 173 8(69)	−0.000 171 12(611)	−0.000 188 33(1248)
γ_{13ll}	−0.003 556(863)	[−0.003 5]	[−0.003 5]	[−0.003 9]
γ_{23ll}	−0.000 836 5(1397)	[−0.000 75]	−0.000 878(252)	−0.001 587(240)
γ_{llll}	0.000 074 15(422)	0.000 072 08(278)	0.000 071 98(234)	0.000 084 29(564)
std. dev. of fit	4.3	2.7	3.4	1.9
number of non-zero weighted measurements:	105	71	62	41

[a] The uncertainty (one standard deviation) in the last digits is given in parentheses.
[b] Values enclosed in square brackets were fixed during the fit.

$$B_v = B_e - \sum \alpha_i(v_i + d_i/2) + \sum\sum \gamma_{ij}(v_i + d_i/2) \times (v_j + d_j/2) + \gamma_{ll}l^2 + \sum\sum\sum \gamma_{ijk}(v_i + d_i/2) \times (v_j + d_j/2)(v_k + d_k/2) + \sum \gamma_{ill}(v_i + d_i/2)l^2 + \gamma_{2222}(v_2 + 1)^4 + \gamma_{2223}(v_2 + 1)^3(v_3 + 1/2) + \gamma_{11ll}(v_1 + 1/2)^2l^2 + \gamma_{22ll}(v_2 + 1)^2l^2 + \gamma_{13ll}(v_1 + 1/2)(v_3 + 1/2)l^2 + \gamma_{23ll}(v_2 + 1)(v_3 + 1/2)l^2 + \gamma_{llll}l^4. \quad [9]$$

The centrifugal distortion constants given in Table 12 were based on fits to the expressions

$$D_v = D_e + \sum \beta_i(v_i + d_i/2) + \sum\sum \beta_{ij}(v_i + d_i/2) \times (v_j + d_j/2) + \beta_{ll}l^2 + \sum \beta_{ill}(v_i + d_i/2)l^2 \quad [10]$$

and

$$H_v = H_e + \sum \epsilon_i(v_i + d_i/2) + \epsilon_{22}(v_2 + 1)^2 + \epsilon_{ll}l^2. \quad [11]$$

The l-type resonance constants were expanded in a similar manner,

$$q_v = q_e + \sum q_i(v_i + d_i/2) + \sum\sum q_{ij}(v_i + d_i/2) \times (v_j + d_j/2) + q_{222}(v_2 + 1)^3 \quad [12]$$

and

$$q_{vJ} = q_{eJ} + \sum q_{iJ}(v_i + d_i/2) + \sum\sum q_{ijJ}(v_i + d_i/2)(v_j + d_j/2). \quad [13]$$

As can be seen in Table 8, there were very few measurements of q_{vJJ} and ρ_v so those measurements were fit to an abbreviated power series

TABLE 12
Centrifugal Distortion Constants in cm^{-1} for Four Isotopomers of HCN

Parameter	$H^{12}C^{14}N$	$H^{13}C^{14}N$	$H^{12}C^{15}N$	$H^{13}C^{15}N$
$D_e\times10^6$	2.858 73(141)[a]	2.718 20(53)	2.693 57(72)	2.561 30(177)
$\beta_1\times10^8$	−3.564 1(1250)	−2.855 7(660)	−3.087 2(720)	−2.938(223)
$\beta_2\times10^8$	6.146 8(1054)	5.955 8(411)	6.223 3(537)	5.499 9(1014)
$\beta_3\times10^8$	0.451 0(1713)	0.581 4(590)	0.652 8(786)	0.570(243)
$\beta_{11}\times10^9$	[0.000]	[0.000][b]	[0.000]	[0.000]
$\beta_{22}\times10^9$	0.749(123)	−0.112(43)	−0.158(49)	0.694(126)
$\beta_{33}\times10^9$	[0.000]	[0.000]	[0.000]	[0.000]
$\beta_{12}\times10^9$	8.693(689)	4.136(452)	6.654(425)	6.253(545)
$\beta_{13}\times10^9$	4.300(1423)	[4.3]	[4.3]	6.15(322)
$\beta_{23}\times10^9$	−0.902(732)	−1.346(298)	−2.92(48)	−3.534(507)
$\beta_{ll}\times10^9$	1.423(433)	−0.853(212)	−0.687(214)	−3.635(356)
$\beta_{lll}\times10^9$	−2.196(469)	−0.188(314)	−1.056(228)	−0.806(222)
$\beta_{2ll}\times10^9$	−0.581(36)	−0.176(14)	−0.158(14)	−0.165(36)
$\beta_{3ll}\times10^9$	[0.700]	−0.089(120)	0.707(220)	1.30(22)
std. dev. of fit	7.3	1.6	2.5	3.5
number of non-zero weighted measurements:	86	62	56	28
$H_e\times10^{12}$	2.356(45)	1.794(35)	1.927(102)	2.071(171)
$\epsilon_1\times10^{12}$	0.182(43)	[0.300]	0.506(134)	0.389(242)
$\epsilon_2\times10^{12}$	0.782(32)	0.766(35)	0.632(79)	0.538(89)
$\epsilon_3\times10^{12}$	[0.0]	[0.0]	[0.0]	[0.0]
$\epsilon_{22}\times10^{12}$	[0.05]	[0.0]	0.050(13)	[0.0]
$\epsilon_{ll}\times10^{12}$	−0.288(13)	−0.211(12)	−0.243(8)	−0.109(29)
std. dev. of fit	2.0	2.0	2.1	3.6
number of non-zero weighted measurements:	31	12	22	11

[a] The uncertainty (one standard deviation) in the last digits is given in parentheses.
[b] Values enclosed in square brackets were fixed during the fit.

$$q_{vJJ} = q^*_{JJ} + q_{2JJ}(v_2 + 1) + q_{3JJ}(v_3 + 1/2) \qquad [14]$$

and

$$\rho_v = \rho^* + \rho_2(v_2 + 1) + \rho_3(v_3 + 1/2). \qquad [15]$$

Those expansion constants are given in Table 13.

EQUILIBRIUM INTERNUCLEAR DISTANCES

We now have enough data to calculate the equilibrium internuclear distances, accurate through all of the quadratic rotational constants and many of the cubic constants, for HCN using eight different isotopomers. Table 11 gives the values of the rotational constants, including B_e, for the isotopomers, $H^{12}C^{14}N$, $H^{13}C^{14}N$, $H^{12}C^{15}N$, and $H^{13}C^{15}N$. The B_e values for the deuterated species are given at the bottom of Table 14. These are slightly different from the values given in Ref. (*1*) because of a computational error that affects only the B_e values in that paper. Until now, the most accurate experimental determination of the equilibrium internuclear distances for HCN was given by Winnewisser *et al.* (*6*) based on the B_e values for only two isotopomers, $H^{12}C^{14}N$ and $D^{12}C^{14}N$. That earlier work used α_i and γ_{ij} constants that were not as accurate as the present values, and for DCN they were significantly different.

Table 11 shows that in most cases the constants for the different isotopomers have nearly the same value. This encouraged us to fix those constants that could not be determined for a certain isotopomer to the value found for a different isotopomer. Thus we were able to use the same model for making the B_e calculation for all isotopomers of HCN. For the DCN isotopomers we could not use the constants for HCN because the isotopic shift was too large. Instead, we concentrated on trying to get as many of the same constants as possible, and on transferring between DCN isotopomers those constants that could only be determined for one or two isotopomers.

In Fig. 4 we give eight lines or curves each of which represents the family of internuclear distances that is compatible with the B_e value for one isotopomer of HCN (or DCN). The crossing points of these lines represent the equilibrium distances for each pair of isotopic B_e values given in Table 14. The four less steeply inclined lines (the dashed lines) are for the deuterated species and the figure shows that their crossing with the more steeply inclined HCN lines gives the best definition of the internuclear distances. The four DCN lines (as well as the HCN lines) are so nearly parallel that small errors in the B_e values can make a large difference in the crossing point and so the internuclear distances are poorly defined. For that reason, one should concentrate attention only on the internuclear distances set off by lines in the lower left-hand corner of the matrix of values given in Table 14. If we use the spread in the internuclear distances as an indication of the uncertainty, the unweighted average distances in HCN are $r_e(\mathrm{CH}) = (1.065\,112 \pm 0.000\,048) \times 10^{-8}$ cm and $r_e(\mathrm{CN}) = (1.153\,283 \pm 0.000\,011) \times 10^{-8}$ cm. These distances are based on unified atomic mass units and other constants all of which are given in Ref. (*9*). The differences shown in Table 14 are within the range of differences expected to arise from inaccuracies in both the data and the model. Carter *et al.* (*10*) used variational calculations to make the B_0–B_e correction. Their values for the equilibrium bond lengths are so close to our values that the uncertainties nearly overlap.

The closeness of the earlier internuclear distances to the present values shows that small differences in the models used to calculate the B_0 to B_e correction are not very important when light atom substitutions are used. They are, however, quite important for heavy atom substitutions. The heavy atom substitutions for DCN show a wider range of internuclear distance solutions than the heavy atom substitutions for HCN, primarily because the data for HCN are more extensive and more accurate, hence the model for calculating the B_0 to B_e correction includes more of the higher order terms and gives a more accurate value for B_e. One is tempted to suggest that the heavy atom substitution for the hydrogen-containing isotopomers gives equilibrium distances that are larger for the CH separation and smaller for the CN separation than the light atom substitutions. However, the uncertainties are large enough to cast doubt on that conclusion.

DISCUSSION

The present results show rather remarkable agreement with the calculated constants given in square brackets in Tables 3 and 4 of our earlier paper (*2*). For the $v_2 = 7$ states the largest difference between our estimated G_c and the present measure-

TABLE 13
The Vibrational Expansion Coefficients in cm^{-1} for the *l*-Type Resonance Constants for Four Isotopomers of HCN

Parameter	$H^{12}C^{14}N$	$H^{13}C^{14}N$	$H^{12}C^{15}N$	$H^{13}C^{15}N$
$q_e \times 10^3$	7.229 287(1837)	6.918 578(3380)[a]	6.815 218(8096)	6.513 317(5063)
$q_1 \times 10^3$	0.089 1(35)	0.094 2(59)	0.101 1(164)	0.096 8(65)
$q_2 \times 10^3$	0.102 71(115)	0.097 9(22)	0.097 58(100)	0.089 8(47)
$q_3 \times 10^3$	−0.021 9(16)	−0.026 8(37)	−0.017 2(145)	−0.029 6(64)
$q_{11} \times 10^4$	−0.162 8(100)	−0.165 6(146)	−0.193 8(256)	[−0.17][b]
$q_{22} \times 10^4$	0.011 69(253)	0.009 24(479)	0.011 08(51)	0.016 03(1142)
$q_{33} \times 10^4$	[0.000]	[0.000]	[0.000]	[−0.000]
$q_{12} \times 10^4$	0.116 57(577)	0.121 7(194)	0.115 4(160)	0.126 5(88)
$q_{13} \times 10^4$	0.788 4(174)	0.796 9(584)	0.872(283)	1.023(121)
$q_{23} \times 10^4$	−0.130 2(53)	−0.140 7(66)	−0.160 8(76)	−0.172 4(61)
$q_{222} \times 10^4$	0.000 61(17)	0.000 68(36)	[0.000 63]	−0.000 1(9)
std. dev. of fit	7.1	3.9	6.9	6.0
number of non-zero weighted measurements:				
	35	20	19	16
$q_{eJ} \times 10^8$	7.763(81)	7.109(45)	6.998(54)	6.374(110)
$q_{1J} \times 10^8$	0.327(141)	0.252(28)	0.470(79)	0.391(52)
$q_{2J} \times 10^8$	0.413(32)	0.376(39)	0.378(26)	0.366(126)
$q_{3J} \times 10^8$	−0.016(106)	0.010(59)	−0.058(65)	−0.087(53)
$q_{11J} \times 10^8$	[0.000]	[0.00]	[0.000]	[0.000]
$q_{22J} \times 10^8$	0.018 9(24)	0.014 6(52)	0.017 5(34)	0.009(18)
$q_{33J} \times 10^8$	[0.000]	[0.000]	[0.000]	[0.000]
$q_{12J} \times 10^8$	0.058(40)	[0.058]	[0.057]	[0.057]
$q_{13J} \times 10^8$	0.491(81)	[0.490]	[0.480]	[0.490]
$q_{23J} \times 10^8$	−0.125(38)	[−0.125]	[−0.115]	[−0.12]
std. dev. of fit	2.8	2.8	3.3	5.1
number of non-zero weighted measurements:				
	27	16	16	14
$q_{JJ}^{*} \times 10^{12}$	1.172(19)		0.968(111)	
$q_{2JJ} \times 10^{12}$	0.092(19)		0.111(9)	
$q_{3JJ} \times 10^{12}$	[0.00]		0.009(222)	
std. dev. of fit	2.3		2.0	
number of non-zero weighted measurements:				
	7		10	
$\rho^{*} \times 10^8$	−1.606(43)	−1.637(24)	−1.493(30)	
$\rho_2 \times 10^8$	−0.089(16)	−0.048(9)	−0.079(10)	
$\rho_3 \times 10^8$	0.045(66)	0.134(37)	0.065(48)	
std. dev. of fit	1.5	0.7	1.9	
number of non-zero weighted measurements:				
	8	7	6	

[a] The uncertainty (one standard deviation) in the last digits is given in parentheses.
[b] Values enclosed in square brackets were fixed during the fit.

ment was 0.022 cm^{-1}, for the 07^70 state. The rotational term values were in equally good agreement.

The present measurements give data for 20 more vibrational energy levels involving the bending mode of $H^{12}C^{14}N$ and yet only a few more constants were needed to produce a fit that was nearly as good as that given in Ref. (*2*). This seems to indicate that the bending vibration is well behaved, which is perhaps not surprising since the Coriolis interactions are quite weak and do not affect the band centers. The bending levels with large *l*-values are too far from other levels with the same symmetry to provide much opportunity for significant vibrational resonance interactions, therefore resonances are more likely to affect the levels with the least vibrational angular momentum. Those problems that do occur in fitting the vibrational and rotational constants to Eqs. [8] and [9] are probably related to the Fermi resonances that have been ignored.

Tables 10–13 show that the heavy atom isotope shifts for most of the constants are not very large. Consequently, one can transfer from one isotope to another those constants that have not been measured and still have confidence that calculated transitions will not be greatly in error provided one is not trying to extrapolate too far outside the range of measurements. The force-field calculations of Strey and Mills (*11*) and Nakagawa and Morino (*12*) are in good agreement with our measurements for the shifts in the lowest order vibrational and rotational constants.

Even though ρ_v and q_l are highly correlated, we still find reasonably good agreement between the values found for the

TABLE 14
Equilibrium Internuclear Distances[a] from B_e Values for Different Pairs of Isotopomers

	$H^{12}C^{14}N$	$H^{13}C^{14}N$	$H^{12}C^{15}N$	$H^{13}C^{15}N$	$D^{12}C^{14}N$[b]	$D^{13}C^{14}N$	$D^{12}C^{15}N$
$H^{13}C^{14}N$	1.065346						
	1.153239						
$H^{12}C^{15}N$	1.065120	1.065521					
	1.153283	1.153206					
$H^{13}C^{15}N$	1.065420	1.065586	1.065550				
	1.153224	1.153194	1.153200				
$D^{12}C^{14}N$	1.065147	1.065158	1.065146	1.065168			
	1.153278	1.153274	1.153278	1.153270			
$D^{13}C^{14}N$	1.065107	1.065122	1.065107	1.065134	1.065577		
	1.153286	1.153281	1.153285	1.153277	1.153130		
$D^{12}C^{15}N$	1.065080	1.065095	1.065081	1.065107	1.066576	1.064447	
	1.153291	1.153286	1.153291	1.153282	1.152785	1.153505	
$D^{13}C^{15}N$	1.065073	1.065091	1.065075	1.065104	1.065636	1.065745	1.065142
	1.153292	1.153287	1.153292	1.153282	1.153109	1.153074	1.153270

[a] The upper entry is r_e(CH) and the lower entry is r_e(CN). All values are given in Ångstrom units, 1×10^{-8} cm. The values are based on unified atomic mass units and I = 505379.0722 / (B (MHz)).
[b] For the deuterated species the following values were used: $B_e(D^{12}C^{14}N)$ = 36 331.985 MHz, $B_e(D^{13}C^{14}N)$ = 35 710.934 MHz, $B_e(D^{12}C^{15}N)$ = 35 289.527 MHz, and $B_e(D^{13}C^{15}N)$ = 34 649.438 MHz.

different isotopomers. Because of the correlation, it is not certain that the isotopic differences are real. One might remark that this work seems to give larger values for ρ_v than our earlier paper, Ref. (*2*). However, if q_l is set to zero, then the values found for ρ_v are close to the values found earlier. The dependence of the ρ_v terms on v_2 is roughly the same for all three isotopomers and probably includes some contribution from q_l which was constrained to have no vibrational dependence.

The relative signs of q_l and ρ_v are determined by the fit of the measurements, but the absolute signs depend on the absolute sign of q_v. Since we have arbitrarily used a positive sign for q_v, then q_l must have a positive sign and ρ_v must be negative. Yamada (*13*) has given a detailed description of how the phase choices affect the sign of q_v. Watson (*5*) gave formulas based on rotational-type contributions in which he showed that if q_l is positive and q_{vJ} is positive, then q_l should be smaller than q_{vJ}. On the contrary, we find that q_l is about 100 times larger than q_{vJ}. Perhaps there are some vibrational-type contributions that are much larger. On the other hand, if a proper analysis were performed with the Fermi resonances taken into account, then the constants might be quite different.

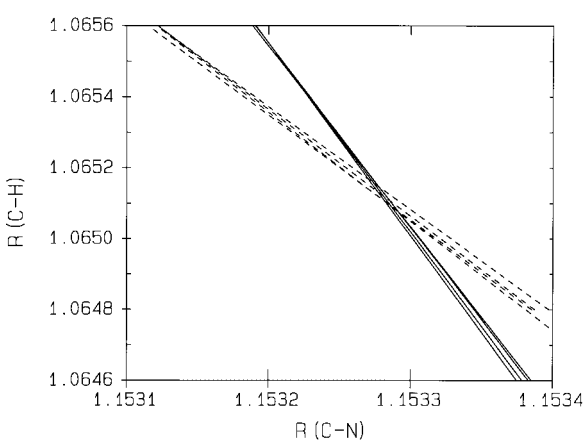

FIG. 4. Plot of the equilibrium internuclear distances in angstrom units (10^{-10} m) compatible with the B_e values for four isotopomers each of HCN and DCN. The solid lines are for HCN and the dashed lines are for DCN. The crossing points for the lines are given in Table 14.

It is somewhat surprising that the power series for the D_v terms fit so poorly for the $H^{12}C^{14}N$ species. Even the D_v terms for the 030 and 040 states are poorly fit, although the fit of the spectroscopic measurements is very good. Table 12 shows that a few constants found for $H^{12}C^{14}N$ are quite different from those for $H^{13}C^{14}N$ and $H^{12}C^{15}N$, even the signs of the β_{ll} terms are different. At first it was believed that the difference was due to the inclusion of data for more of the higher stretching states. To test that possibility we tried a fit in which the only data used were for vibrational states observed in both $H^{12}C^{14}N$ and $H^{13}C^{14}N$. That fit gave nearly the same constants as given in Table 12 and again the standard deviation of the fit for $H^{12}C^{14}N$ was quite poor. Since the centrifugal distortion terms are sensitive to weak interactions, the poor fit of the $H^{12}C^{14}N$ centrifugal distortion terms may be due to interactions that were not taken into account in our analysis, especially the possibility of Fermi resonance.

There are surprisingly large vibrational (or l-dependent) shifts for some of the higher order constants such as H_v and q_{vJ}. For example, B_v changes by less than 2% as l changes from 1 to 9 with no change in the vibrational quantum numbers, while H_v changes by more than a factor of 10.

Note on Supplemental Data

An extensive listing of the data used in the least-squares analysis is available from the authors in the form of a diskette containing *ASCII* files for Tables A-1, A-2, and A-3. These files are also available as supplementary data on the journal home page (http://www.academicpress.com/jms).

ACKNOWLEDGMENTS

We thank Brenda P. Winnewisser for valuable comments on the manuscript. Financial support of the Deutsche Forschungsgemeinschaft is gratefully acknowledged.

REFERENCES

1. W. Quapp, M. Hirsch, G. C. Mellau, S. Klee, M. Winnewisser, and A. Maki, *J. Mol. Spectrosc.* **195,** 284–298 (1999).
2. A. Maki, W. Quapp, S. Klee, G. C. Mellau, and S. Albert, *J. Mol. Spectrosc.* **180,** 323–336 (1996).
3. A. Maki, W. Quapp, and S. Klee, *J. Mol. Spectrosc.* **171,** 420–434 (1995).
4. A. G. Maki and J. S. Wells, "Wavenumber Calibration Tables from Heterodyne Frequency Measurements," NIST Special Publication 821, U.S. Government Printing Office, Washington, D.C., 1991. [also available in updated form via the internet at http://physics.nist-.gov/]
5. J. K. G. Watson, *J. Mol. Spectrosc.* **101,** 83–93 (1983).
6. G. Winnewisser, A. G. Maki, and D. R. Johnson, *J. Mol. Spectrosc.* **39,** 149–158 (1971).
7. J. Preusser and A. G. Maki, *J. Mol. Spectrosc.* **162,** 484–497 (1993).
8. F. J. Lovas, *J. Phys. Chem. Ref. Data* **7,** 1445–1750 (1978).
9. Ian Mills, "Quantities, Units, and Symbols in Physical Chemistry," International Union of Pure and Applied Chemistry, Physical Chemistry Division, Blackwell Scientific Publications, Oxford, 1989.
10. S. Carter, I. M. Mills, and N. C. Handy, *J. Chem. Phys.* **93,** 1606–1607 (1992).
11. G. Strey and I. M. Mills, *Mol. Phys.* **26,** 129–138 (1973).
12. T. Nakagawa and Y. Morino, *J. Mol. Spectrosc.* **31,** 208–229 (1969).
13. K. Yamada, *Z. Naturforsch., A: Phys. Sci.* **38,** 821–834 (1983).